Journal of Inflammation Research Dovepress

Open Access Full Text Article ORIGINAL RESEARCH

Integrated Small Intestine Microbiota and Serum Metabolomics Reveal the Potential Mechanisms of Wine Steaming in Alleviating Rhubarb-Induced Diarrhea

Ya-Ya Bai[1], Rui Tian[1], Yan Qian[2], Qiao Zhang[1], Chong-Bo Zhao[1], Yong-Gang Yan[1], Li Zhang[3], Shi-Jun Yue[4], Yu-Ping Tang[1]

[1]Key Laboratory of Shaanxi Administration of Traditional Chinese Medicine for TCM Compatibility, and State Key Laboratory of Research & Development of Characteristic Qin Medicine Resources (Cultivation), and Shaanxi Collaborative Innovation Center of Chinese Medicinal Resources Industrialization, and Shaanxi Traditional Chinese Medicine Processing Technology Heritage Base, Shaanxi University of Chinese Medicine, Xi'an, 712046, People's Republic of China; [2]Suzhou Institute for Drug Control, Suzhou, Jiangsu Province, 215000, People's Republic of China; [3]Hanlin College, Nanjing University of Chinese Medicine, Taizhou, Jiangsu Province, 225300, People's Republic of China; [4]International Joint Research Center on Resource Utilization and Quality Evaluation of Traditional Chinese Medicine of Hebei Province, Hebei University of Chinese Medicine, Shijiazhuang, 050200, People's Republic of China

Correspondence: Qiao Zhang, Shaanxi University of Chinese Medicine, Shiji Avenue, Xi Xian New District, Xi'an, 712046, People's Republic of China, Tel +86-15895973680, Fax: +86-02938185061, Email 18700081184@163.com

Background: Long-term use of rhubarb (RH) commonly leads to diarrhea, which can be alleviated by steaming with wine. However, the specific mechanism by which wine steaming alleviates RH-induced diarrhea remains unknown.

Objective: This study aims to reveal the underlying mechanisms of wine steaming in alleviating RH-induced diarrhea by examining small intestinal flora and serum metabolomics.

Methods: Major anthraquinone and anthrone components were detected using ultra-performance liquid chromatography-mass spectrometry (UPLC-MS). Eighty-four ICR mice were randomly divided into control, RH, and RH steamed with wine (PRH) groups and were administered RH and PRH (1, 4, and 8 g/kg, i.g). for 14 consecutive days. Histopathological analysis was performed using hematoxylin-eosin staining. Levels of inflammatory factors and tight junction proteins, zonula occludens-1 (ZO-1) and occludin, in the small intestine were measured. The small intestine content was analyzed using 16S rRNA sequencing, and UPLC-MS was used to analyze endogenous metabolites.

Results: Levels of major anthraquinone and anthrone components decreased in PRH. Both RH and PRH groups showed varying degrees of loose stools and increased fecal water rates; the RH group exhibited more severe effects. Compared with the control group, RH caused small intestine injuries, increased levels of inflammatory cytokines, downregulated the expression of ZO-1 and occludin, and induced gut microbiota (GM) imbalance. The relative abundance of *Lactobacillus* decreased, while the relative abundance of *Shigella* and *Streptococcus* increased. However, PRH had a milder impact than RH. The glycerophospholipid metabolic pathway was involved in this effect. The levels of inflammatory cytokines and potential metabolites (sn-glycero-3-phosphoethanolamine) were positively correlated with *Streptococcus* infection, while the levels of ZO-1 and occludin were negatively correlated with *Streptococcus* infection. GM imbalance and abnormal glycerophospholipid metabolism contributed to impaired intestinal barrier function and inflammatory factor release, which may underlie RH-induced diarrhea, though PRH had a weaker effect.

Conclusion: PRH alleviated RH-induced diarrhea by recovering GM balance, reducing ZO-1 and occludin expression, and decreasing the release of inflammatory factors. This mechanism may be linked to the reduced anthraquinone content. This study is the first to explore the mechanism of wine steaming in alleviating RH-induced diarrhea through small intestinal flora and serum metabolomics. It provides data to support the broader clinical use of RH and its safer application.

Keywords: gut microbiota, metabolomics, wine steaming, diarrhea, rhubarb

Received: 24 May 2024
Accepted: 17 October 2024
Published: 30 October 2024

Graphical Abstract

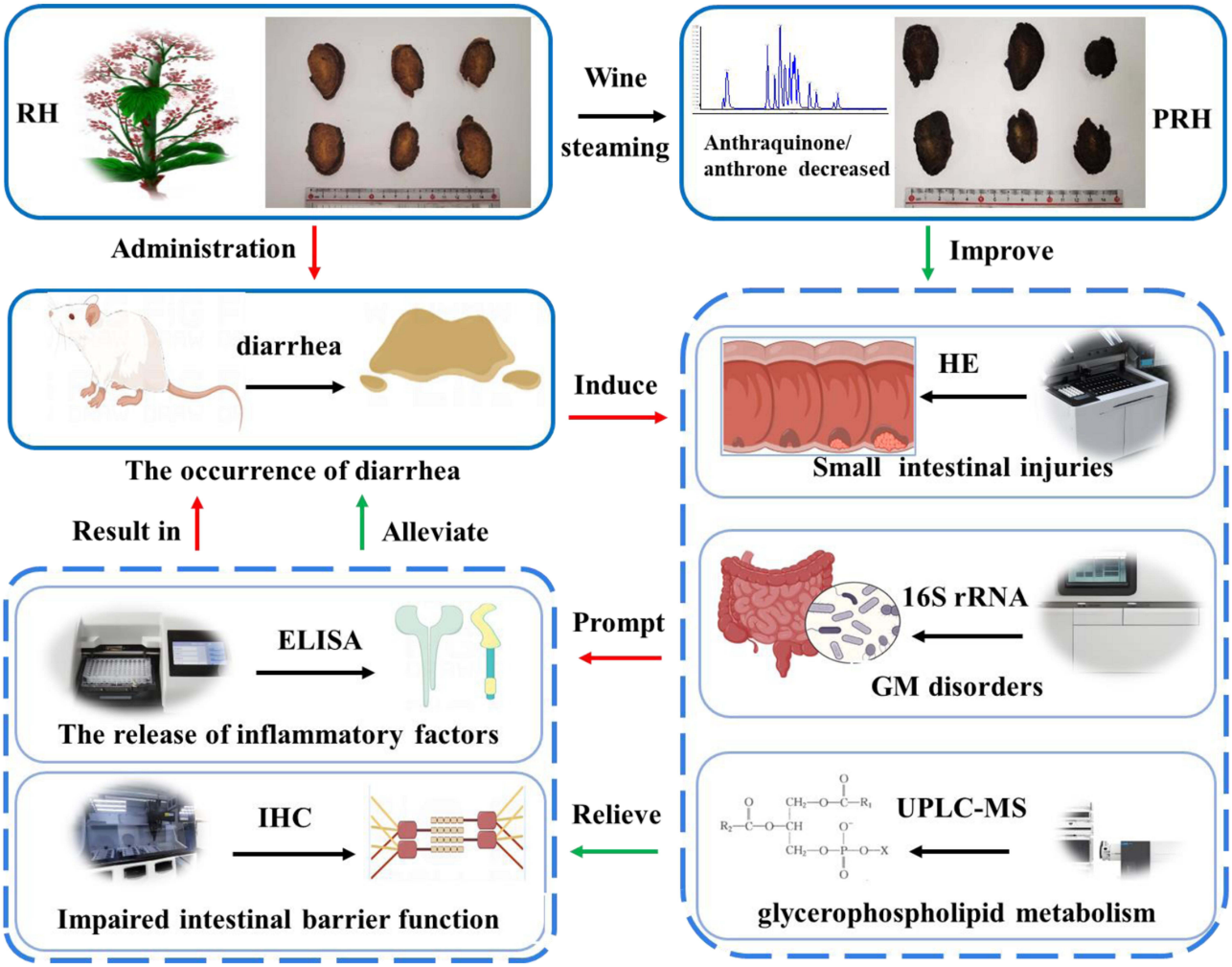

Introduction

Traditional Chinese medicine (TCM) has been used for thousands of years to treat and prevent diseases, though some exhibit certain adverse reactions that are attracting increasing attention.[1] Rhubarb (RH) is the dried root and rhizome of *Rheum palmatum* L., *R. tanguticum* Maxim. ex Balf., and *R. officinale* Baill., as recorded in Shennong's Herbal Classic (Shennong-Bencao Jing). It has been commonly used in China to treat constipation, amenorrhea, and edema.[2] However, modern pharmacological studies have shown that the long-term use of RH commonly leads to a series of gastrointestinal adverse reactions, including symptoms such as diarrhea, abdominal pain, and vomiting, which are related to the "cold property" of RH.[3,4] The "cold property" is one of the four properties (cold, hot, warm, and cool) in TCM, reflecting the unique influence of TCM on the body.[5] Thus, RH must be processed before being used to treat constipation in clinics, and steaming with wine is a common method used to alleviate the side effects (diarrhea) caused by the excessive "cold property" of RH in clinical practice.[6]

TCM can cause different changes after processing, such as reduced toxicity, increased efficacy, or property conversion.[7–9] Wine has been used as a processing material in TCM for thousands of years, with yellow rice wine (Chinese: 黄酒) being used in TCM processing without special regulations according to the 2020 edition of the Chinese

Pharmacopoeia.[10] Many "cold" Chinese medicines show reduced side effects and enhanced efficacy after being processed by wine. For example, after being stir-fried with wine, the bitter and cold nature of *Radix scutellariae* is alleviated, and the efficacy of clearing heat is enhanced. After being processed with wine, *Coptis* could relieve coldness and enhance its therapeutic effect on gastric ulcer in rats.[11,12] RH is one of the most commonly used TCMs in clinical practice, and steaming with wine aims to alleviate its 'cold property,' reduce diarrhea, and promote blood circulation.[13] The medicinal property of RH is cold, while wine is hot, and steaming RH with wine (PRH) fits into the theory of 'heat restraining cold,' which aligns with its clinical applications in TCM. While there is limited literature specifically assessing the diarrhea-inducing effects of RH before and after wine steaming, existing studies suggest that the diarrhea effect of PRH decreases, which may be related to the inhibition of inflammatory factors.[5,14] Additionally, anthraquinones in RH have a purgative effect, and changes in the ingredients of RH occur after wine steaming,[15] However, the specific changes in the ingredients and the mechanism by which diarrhea is induced by RH remain unclear. Therefore, the underlying mechanisms must be further elucidated.

Diarrhea is a common functional gastrointestinal disease with a complex pathogenesis.[16] Liver, gallbladder, and gastrointestinal diseases, bacterial or viral infections, malabsorption, and chronic inflammatory diseases can all lead to the occurrence and development of diarrhea.[17] Emerging clinical and basic evidence strongly supports that gut microbiota (GM) plays an important role in maintaining host health.[18] Under normal physiological conditions, the structure and composition of GM remain in stable balance, performing functions like metabolism, immunity, and maintaining the stability of the intestinal barrier.[19] However, under pathological conditions, GM is severely damaged, with an increase in pathogenic bacteria (eg, *Escherichia coli*) and a decrease in probiotics (eg, *Bifidobacterium* and *Lactobacillus*).[20] Studies have reported that the occurrence and development of diarrhea is often accompanied by GM dysbiosis, causing a decrease in beneficial bacteria and an increase in pathogenic bacteria. In addition, GM dysbiosis involves decreased intestinal immune function and the release of pro-inflammatory factors.[21] GM changes play a prominent role in the occurrence of diarrhea.

Metabolomics has been widely used for diagnosing and monitoring diseases.[22] It provides potential biomarkers related to cardiovascular and inflammatory diseases, intestinal cancer, and other chronic diseases.[23,24] Research has shown that GM changes are involved in the physiological and pathological processes of the body, particularly in regulating metabolism and immunity.[25] Therefore, more attention and research into GM may contribute to revealing the mechanism by which wine steaming alleviates diarrhea induced by RH.

This study explored the mechanism by which RH alleviates diarrhea after wine steaming, focusing on GM and serum metabolomics. Simultaneously, ultra-performance liquid chromatography-mass spectrometry (UPLC-MS) was used to quantitatively analyze the differential components of RH and PRH to clarify the possible material basis for the alleviation of diarrhea after RH steaming, aiming to provide data supporting the clinical safety of RH.

Materials and Methods

Reagents

The dried roots of RH were collected from Gan Nan, Gansu Province, China, and identified as *R. tanguticum* by Prof. Yong Gang Yan (Shaanxi University of Chinese Medicine, Xianyang 712046, China). A voucher specimen (20220812) was deposited in the Herbarium of the College of Pharmacy, Shaanxi University of Chinese Medicine (Xi'an, China). The cleaned RH was immersed in yellow rice wine (100:30), moistened thoroughly, set in a steaming container, and steamed until black inside and outside. It was then removed, cooled, dried, and referred to as PRH (Figure S1). Both RH and PRH were crushed into powder (65-mesh).

The RH powder was immersed in water (1:8) for 30 min, heated, and boiled for 3 min. After filtration, the residue was decocted twice in water (1:8) for 3 min. Finally, the filtrates were combined three times, reduced to 1 g/mL at 45°C, and stored at −20°C until further use.

Animals and Groups

Male ICR mice (20 ± 2 g, SPF grade) were purchased from Chengdu Dashuo Experimental Animal Co. Ltd. (License No. SCXK (川) 2020–030). The experimental protocols were approved by the Animal Experimental Ethical Committee of Shaanxi University of Chinese Medicine (No. SUCMDL20210310004), and all experiments conformed to the "Guidelines for the Care and Use of Laboratory Animals."[26]

Eighty-four ICR mice were randomly divided into the control group (Control), high (RH-H), medium (RH-M), and low (RH-L) dose groups of RH, and high (PRH-H), medium (PRH-M), and low (PRH-L) dose groups of PRH. The RH and PRH groups were converted based on clinical daily dosage (5 g) and administered as water extract (equal, four, and eight times; 1, 4, and 8 g/kg, i.g). The control group was administered an equal volume of salt solution (0.9%) once a day for 14 consecutive days.

Fecal Morphology Observation and Determination of Fecal Water Rate

The mental state, behavioral activity, and fecal morphology of the mice were observed during administration. The fecal water rate of the mice was calculated on days 7 and 14 after administration as follows:

$$\text{Fecal water rate } (\%) = (\text{wet weight} - \text{dry weight})/\text{wet weight} \times 100\%$$

Histopathology of the Small Intestine

An appropriate amount of small intestine was placed into 4% neutral polyformaldehyde (Guo Yao Group Chemical Reagent Co., Ltd, No. 20210122), embedded in paraffin, and stained with hematoxylin-eosin (HE). The slices were imaged under a microscope for pathological observation (Leica, Berlin, Germany).

Detection of Tumor Necrosis Factor Alpha (TNF-α), Interleukin-6 (IL-6), and Interferon Gamma (IFN-γ)

Total protein levels were determined using a bicinchoninic acid protein assay kit (Jiancheng, Nanjing, China), and TNF-α, IL-6, and IFN-γ levels in the small intestine were measured using enzyme-linked immunosorbent assay kits (No: A0119, A0107, A0124, Jiancheng, Nanjing, China).

Determination of Zonula Occludens-1 (ZO-1) and Occludin Expression Using Immunohistochemistry (IHC)

Paraffin-embedded small intestine tissues were deparaffinized in xylene and washed with ethanol (gradient elution), as previously described.24 The intestinal sections were then treated with 3% H_2O_2 for 30 min at 37°C, immune-blocked, and incubated overnight at 4°C with primary antibodies (ZO-1 1:500; occludin 1:600). Next, the sections were incubated with horseradish peroxidase-labeled secondary antibody for 90 min. The slices were observed using SlideViewer 2.6, and mean density was measured using Image-Pro Plus 6.0 (IPP 6.0, Media Cybernetics, USA) software.

DNA Extraction from the Small Intestine Content and 16S rRNA Sequencing

DNA from the content of the small intestine was extracted using the OMEGA Soil DNA Kit (Omega Bio-Tek, Norcross, GA, USA) according to the manufacturer's instructions and stored at −20°C for further analysis. The quantity and quality of the extracted DNA were determined using a NanoDrop NC2000 spectrophotometer (Thermo Fisher Scientific, Waltham, MA, USA) and agarose gel electrophoresis.

The forward primer 338F (5′-ACTCCTACGGGAGGCAGCA-3′) and reverse primer 806R (5′-GGACTACHVGGGTWTCTAAT-3′) were used for polymerase chain reaction (PCR) amplification of the bacterial 16S rRNA gene V3-V4 region. The PCR amplicons were purified and quantified using Vazyme VAHTSTM DNA Clean Beads (Vazyme, Nanjing, China) and the Quant-iT PicoGreen dsDNA Assay Kit (Invitrogen, Carlsbad, CA, USA), respectively. Purified amplicons were pooled in equal amounts, and paired-end 2×250 bp sequencing was performed on an Illumina NovaSeq platform.

Serum Metabolomics

Serum (50 μL) was added to 400 μL of acetonitrile and methanol (1:1) (Merck, Darmstadt, Germany), after thawing at 4°C. The mixture was vortexed for 30s, sonicated at 40 kHz for 30 min at 5°C, and centrifuged at 13,000 rpm for 10 min at 4°C. Three hundred microliters of supernatant was collected and concentrated to dryness at 30°C. The dried residues were redissolved in acetonitrile and water (1:1), vortexed for 30s, and centrifuged at 13,000 rpm for 10 min at 4°C. The supernatant was used for subsequent analyses.

UPLC-MS analysis was performed using the Vanquish Horizon UHPLC System and a Q-Exactive HF-X mass spectrometer (Thermo Scientific, MA, USA). An ACQUITY UPLC HSS T3 column (100 mm × 2.1 mm, 1.8 μm; Waters, Milford, USA) was used, with the column temperature set at 40°C. The mobile phase consisted of A (0.1% formic acid in water and acetonitrile, 95:5) and B (0.1% formic acid in isopropanol, acetonitrile, and water, 9.5:9.5:1), with a gradient elution as follows: 0–3 min, 0–20% B; 3–4.5 min, 20–35% B; 4.5–5 min, 35–100% B; 5–6.3 min, 100–100% B; 6.3–6.4 min, 100–0% B; 6.4–8 min, 0–0% B. The flow rate was 0.4 mL/min, and the injection volume was 3 μL.

The heater temperature and voltage were maintained at 425°C and 3500 V (positive), 3500 V (negative), respectively. The detailed parameters were as follows: sheath gas flow rate was maintained at 50 arb, auxiliary gas flow rate at 13 arb, capillary temperature at 325°C, S-Lens radio frequency level at 50 V, and collision energy at 40 eV.

Quantitative Analysis of Anthraquinones and Anthrones in RH and PRH

The compounds Sennoside B (**1**, No. 19120607), Rhein-8-*O*-*β*-D-glucopyranoside (**2**, No. 17101705), Emodin-8-*O*-*β*-D-glucopyranoside (**3**, No. 19102903), Aloe-emodin-3-(hydroxymethyl)-*O*-*β*-D-glucopyranoside (**4**, No. PS1495), Chrysophanol-8-*O*-*β*-D-glucoside (**5**, No. 6473), Physcion-8-*O*-*β*-D-glucopyranoside (**6**, No. B20243), Aloe emodin (**7**, No. 150730), Emodin (**8**, No. 150526), Chrysophanic acid (**9**, No. 151028), and Physcion (**10**, No. AF8041803) were obtained from Yuanye Company (Shanghai, China), with a purity ≥ 98%.

Quantitative analysis was performed using UPLC-MS (DGU-20A5R, Shimadzu, Kyoto, Japan; AB Sciex Turboionspray®, AB Sciex, MA, US). ACQUITY UPLC® BEH C18 (100 mm × 2.1 mm, 1.7 μm; Waters, Milford, USA) was applied with a column temperature of 35 °C. The mobile phase was composed of A (5 mmol ammonium acetate aqueous solution) and B (100% acetonitrile) with a gradient elution as follows: 0–0.5 min, 10%B; 0.5–4 min, 10%-96%B; 4–5 min, 96%-96%B; 5–5.5 min, 96%-10%B, 5.5–7 min, 10%B. The flow rate and injection volume were 0.3 mL/min and 10 μL, respectively.

Negative mode and multiple reaction monitoring (MRM) mode were used for quantitative analysis. The temperature and voltage of the ion source were maintained at 550 °C and −4500V, respectively. Collisionally activated dissociation, 10 psi; Curtain Gas, 10 psi; Ion Source Gas1, 60 psi; Ion Source Gas2, 60 psi.

Statistical Analyses

Statistical analyses were performed using GraphPad Prism 7 software (San Diego, CA, USA). One-way analysis of variance, followed by Dunn's multiple comparison tests, was used for analysis. Data are expressed as means ± standard deviation (SD), and $p < 0.05$ was considered statistically significant.[24,27]

Results

Observation of Fecal Morphology and Determination of Fecal Water Rate

No deaths occurred during the experiment, and the control group exhibited good mental state, shiny fur, and normal fecal morphology. In contrast, the administration groups displayed signs of mental exhaustion, dirty perianal areas, loose stools, and in some cases, semiliquid stools (Figure S2). The fecal morphology for each group is shown in Figure S3. Compared with the control group, the feces of the administration groups showed varying degrees of looseness. The fecal water rate of each group is depicted in Figure 1; compared to the control group, the fecal water rate significantly increased in the RH-H, RH-M, and PRH-H groups on day 7 (first week, F-W) and day 14 (second week, S-W). Additionally, in comparing fecal water rates between F-W treatment groups, the rates were significantly higher in the RH-H and RH-M groups. These findings indicate that RH induces diarrhea in mice, while the effect of PRH is milder than RH.

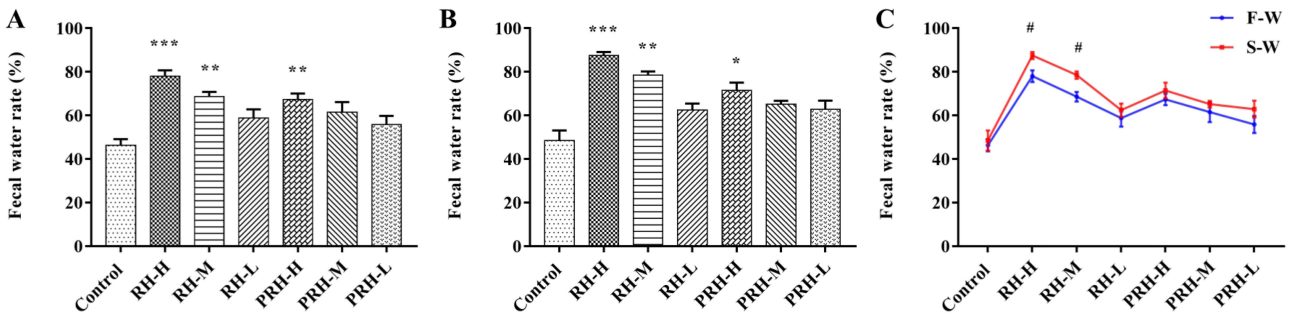

Figure 1 Effects of each group on fecal water rate (n = 6) (**A**) F-W, compared with control group, $^{**}p < 0.01$, $^{***}p < 0.001$; (**B**) S-W, compared with control group, $^{*}p < 0.05$, $^{**}p < 0.01$, $^{***}p < 0.001$; (**C**) compared with the corresponding two groups on the F-W and S-W, $^{\#}p < 0.05$).

HE Staining

As shown in Figure 2, the intestinal mucosal structure in the control group remained intact. In contrast, different degrees of mucosal epithelial necrosis and minimal fibrous tissue proliferation were observed in the RH and PRH F-W groups.

The extent of tissue damage in the RH and PRH groups exacerbated with prolonged administration, as indicated by vascular congestion and the presence of neutrophils. Notably, compared to the RH groups, the pathological changes in the

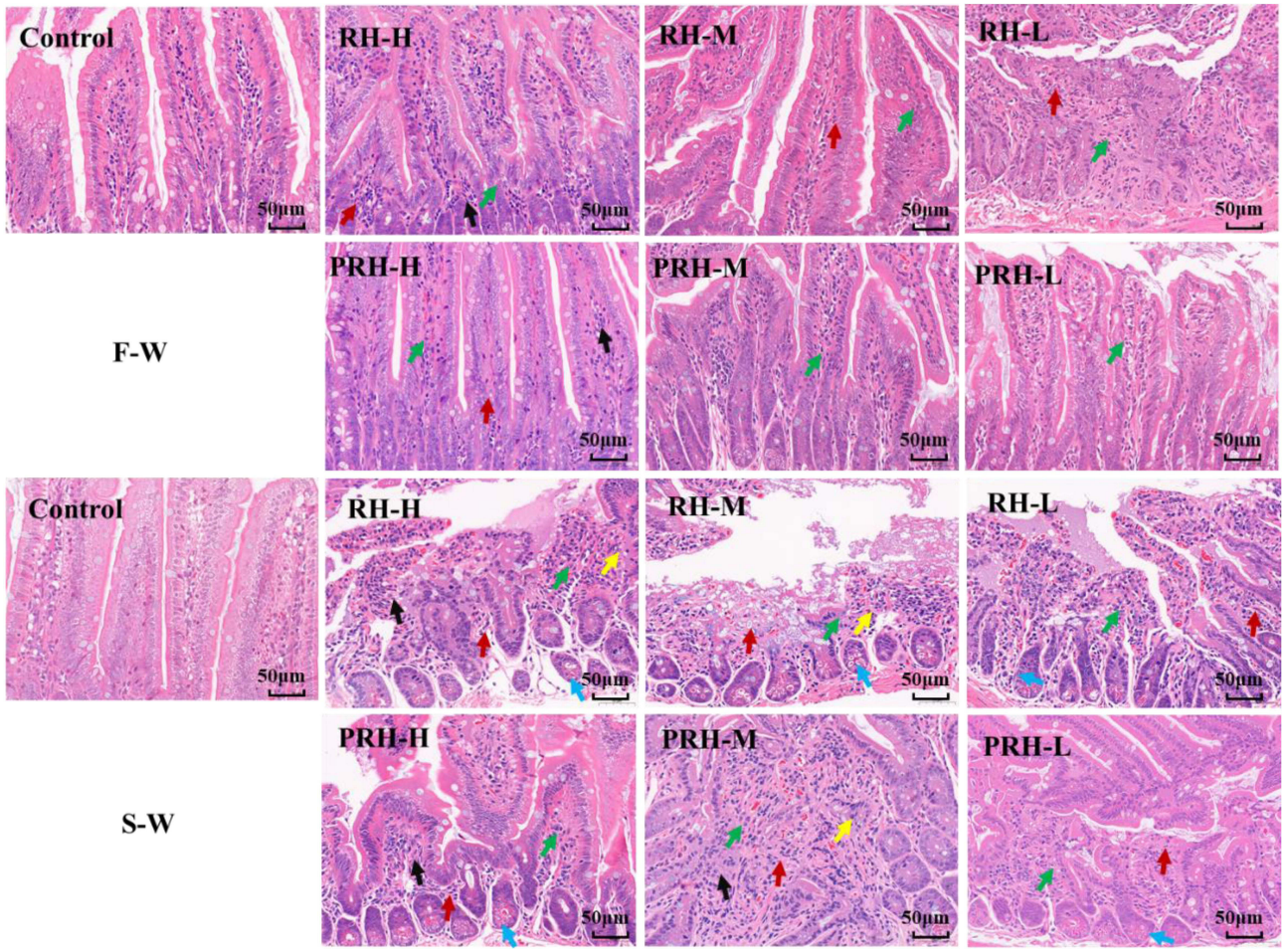

Figure 2 HE staining of small intestine. (Scale bar: 50 μm, green arrow, mucosal epithelial necrosis; blue arrow, vascular congestion; black arrow, fibroblasts; red arrow, fibrocyte; yellow arrow, neutrophils).

PRH groups were less severe. These results demonstrate that both RH and PRH caused small intestinal tissue damage, although the effect of PRH was relatively weaker.

Determination of TNF-α, IL-6, and IFN-γ Levels

As shown in Figure 3A, the levels of TNF-*α*, IL-6, and IFN-*γ* were significantly elevated in the high- and medium-dose groups of both RH and PRH, with no significant changes observed in the RH-L and PRH-L groups. Additionally, IFN-γ levels were significantly reduced in the PRH-H and PRH-M groups compared to all dose groups of RH. Furthermore, IL-6 levels were significantly reduced in the PRH-H group, while no significant changes were observed in the other groups.

Compared to the control group, TNF-α and IFN-γ levels were significantly increased in the high- and medium-dose groups of both RH and PRH. Additionally, TNF-α and IL-6 levels increased in the RH-L and PRH-H groups, respectively. Compared with all dose groups of RH, TNF-*α* and IFN-*γ* levels were significantly reduced in the PRH-H and PRH-M groups, with no significant changes in the other groups (Figure 3B).

As shown in Figure 3C, compared with all F-W dose groups, TNF-*α* and IFN-*γ* levels significantly increased in the RH-H and RH-M groups in S-W, while IL-6 levels increased in the RH-H, RH-M, and PRH-H groups.

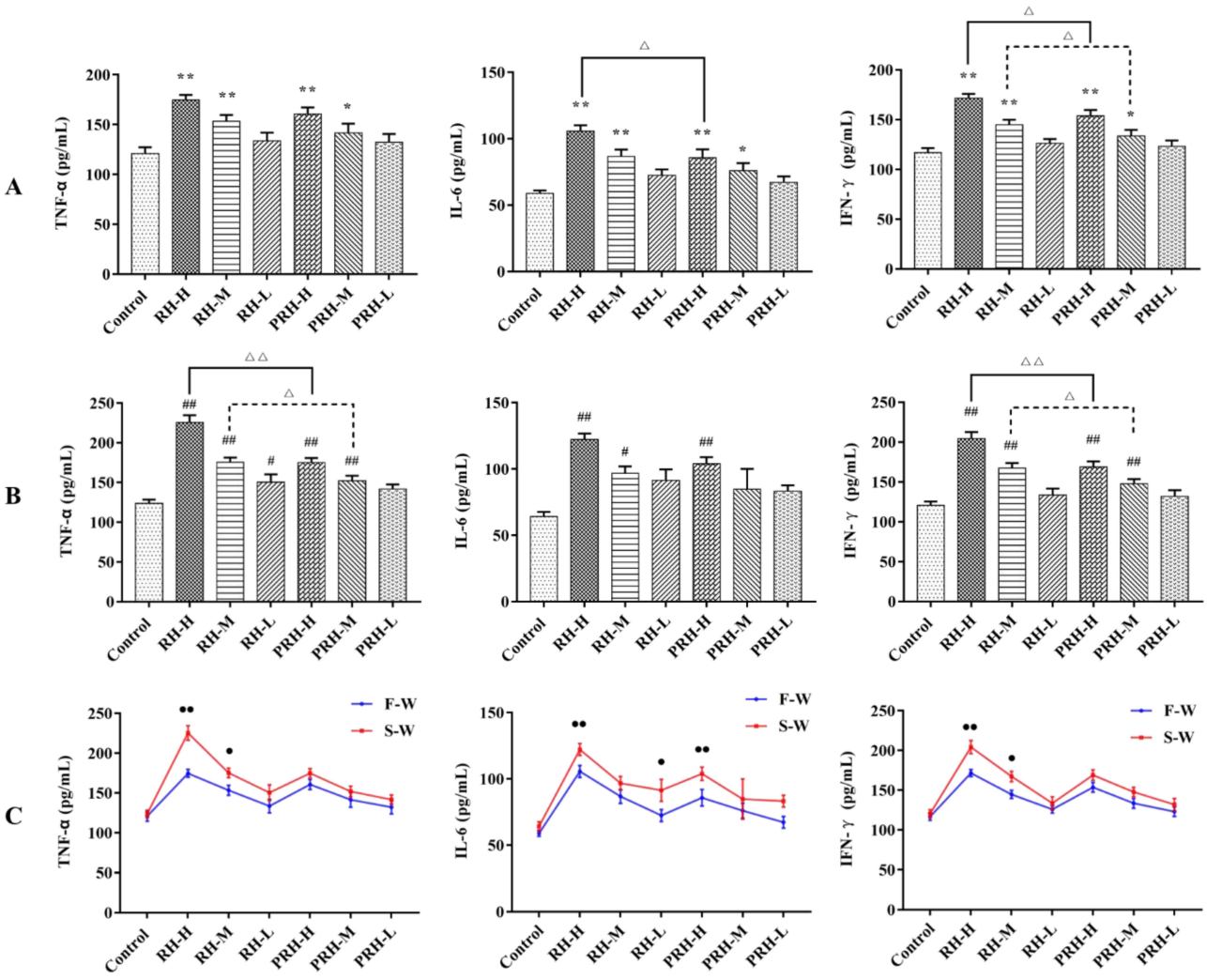

Figure 3 Effects of each group on TNF-*α*, IL-6 and IFN-*γ* (n = 6) (**A**) F-W, compared with control group, **p* < 0.05, ***p* < 0.01; Comparison of RH and PRH dose groups, $^{\Delta}p < 0.05$, $^{\Delta\Delta}p < 0.01$; (**B**) S-W, compared with control group, $^{\#}p < 0.05$, $^{\#\#}p < 0.01$; Comparison of RH and PRH dose groups, $^{\Delta}p < 0.05$, $^{\Delta\Delta}p < 0.01$; (**C**) compared with the corresponding two groups on the F-W and S-W, $^{\bullet}p < 0.05$, $^{\bullet\bullet}p < 0.01$).

These results suggest that both RH and PRH elevate inflammatory factor levels in mice, but PRH has a weaker effect than RH. Moreover, prolonged administration of RH and PRH exacerbated the inflammatory response in mice.

Occludin and ZO-1 Expression in the Small Intestine

all intestinal injury, and inflammatory factor levels observed with prolonged administration, IHC analysis of the small intestine was performed to further assess the effects of RH and PRH.

Compared with the control group, the protein expression of occludin and ZO-1 significantly decreased in the high-dose RH and PRH groups, with occludin expression also significantly reduced in the RH-M group. Although not statistically significant, the reduction in the PRH groups was less pronounced compared to the RH groups (Figure 4).

Effect of RH-H and PRH-H on Small Intestinal Microbiota

The results from fecal water rate measurement, HE staining, inflammatory factor measurement, and IHC staining demonstrated that RH and PRH intensified effects on various indicators in mice during S-W. Additionally, a dose-dependent effect was observed among the high-, medium-, and low-dose RH and PRH groups, with significant differences in the high-dose RH and PRH groups. Therefore, we focused on high-dose RH and PRH groups for GM analysis.

According to different groups, amplicon sequence variant/operational taxonomic unit (OTU) analysis was performed after high-throughput sequencing using Illumina. As shown in Figure 5A, there are 1868 OTUs in the control group, 2110 OTUs in the RH-H group, and 1533 OTUs in the PRH-H group. These results indicate a significant difference in GM structure among the groups. The rarefaction curve directly reflects the rationality of the sequencing data and indirectly reflects species richness within the sample. The rarefaction curves of each group tend to flatten out, indicating that the sequencing data are sufficient and can reflect the microbial diversity information in the samples (Figure 5B).

The alpha diversity of the GM in the samples was analyzed using the Chao 1 and Shannon indices (Figure 5C). These indices showed that, compared to the control group, the richness and diversity of the microbial community in the RH-H group increased, although not significantly. No significant changes were observed in the PRH-H group. The beta diversity of the GM in the samples was analyzed using principal coordinate analysis (Figure 5D). The distance between samples in the control, RH-H, and PRH-H groups was relatively small, while significant differences in GM composition were observed between the RH-H and PRH-H groups compared to the control group.

The species composition analysis is shown in Figure 6A and B. At the phylum level (Figure 6A), Firmicutes, Bacteroidetes, and Proteobacteria were the main species in each group, with a relative abundance of over 90%. Compared with the control group, the proportion of Firmicutes increased in the RH-H group, which was higher than that of the PRH-H group. The proportion of Bacteroidetes did not change significantly in the RH-H group, while it increased in the PRH-H group. The proportions of Proteobacteria decreased in both the RH-H and PRH-H groups. At the genus level (Figure 6B), *Lactobacillus, Streptococcus, Allobaculum*, and *Adlercreutzia* were the main bacterial genera in each group. Compared to the control group, the relative abundance of *Lactobacillus* decreased in the RH-H group, and the proportion of reduction was higher than that in the PRH-H group; the relative abundance of *Streptococcus* was higher in the RH-H group than in the PRH-H group, while the relative abundances of *Allobaculum* and *Adlercreutzia* were lower in both the RH-H and PRH-H groups.

The results of the linear discriminant analysis effect size difference analysis are shown in Figure 6C and D. At the genus level, the abundance of *Streptococcus, Shigella, Phascolarctobacterium*, and *Helicobacter* increased in the RH-H group compared to the control group, while the abundance of *Adlercreutzia, Desulfovibrio, Acinetobacter, Limnohabitans*, and *Stenotrophomonas* decreased in the RH-H group (Figure 6C). Compared to the control group, the abundance of *Streptococcus, Ruminococcus, Akkermansia, Phascolarctobacterium*, and *Blautia* increased in the PRH-H group, while the abundance of *Desulfovibrio, Acinetobacter, Pediococcus*, and *Limnohabitans* decreased in the RH-H group (Figure 6D). The increase in *Streptococcus* abundance in the PRH-H group was less pronounced than that in the RH-H group.

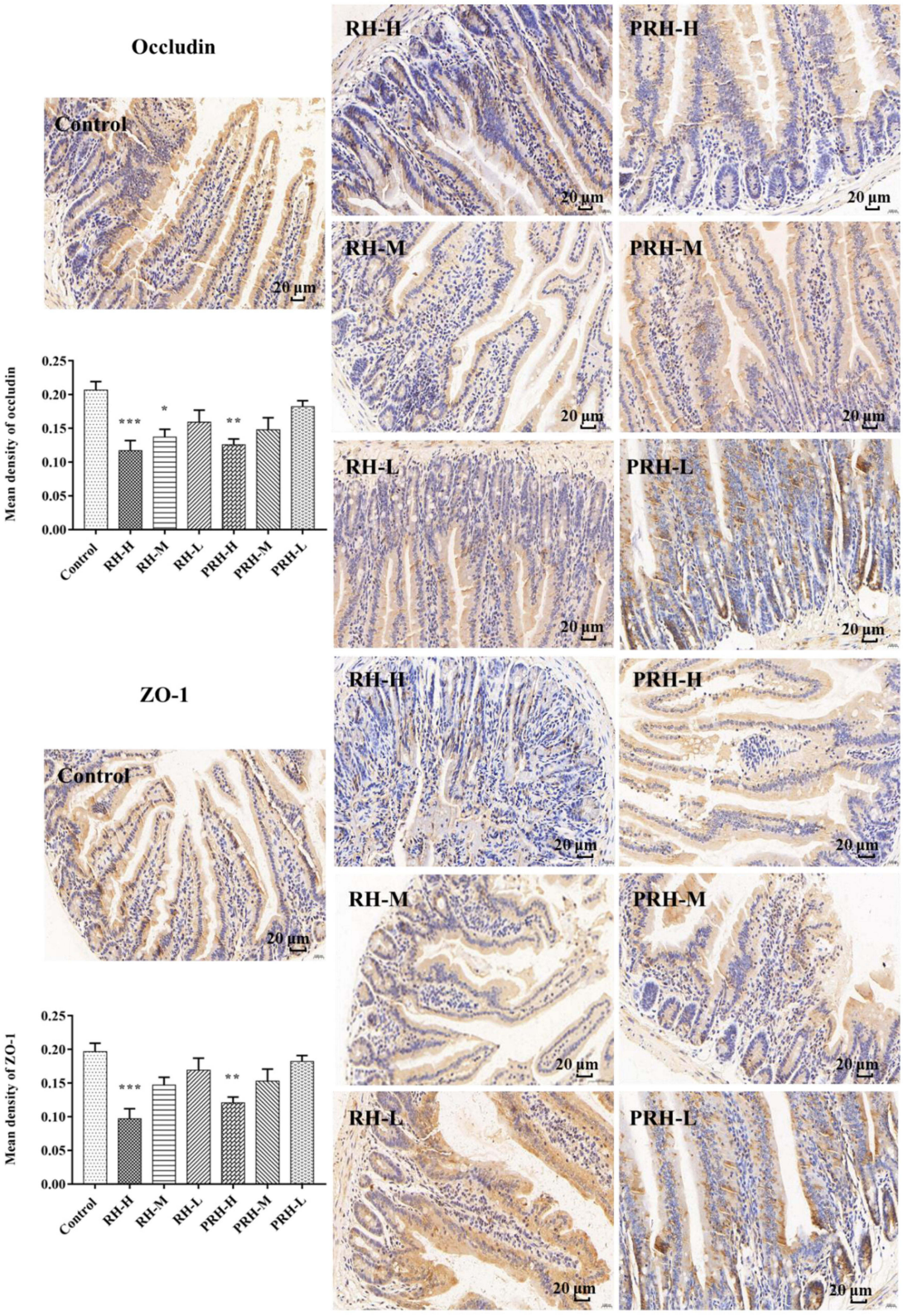

Figure 4 IHC determined the expression of small intestine (occludin and ZO-1, Scale bar: 20 μm), data are expressed as mean ± SD (n= 6, *p < 0.05, **p < 0.01, ***p < 0.001, compared to control group).

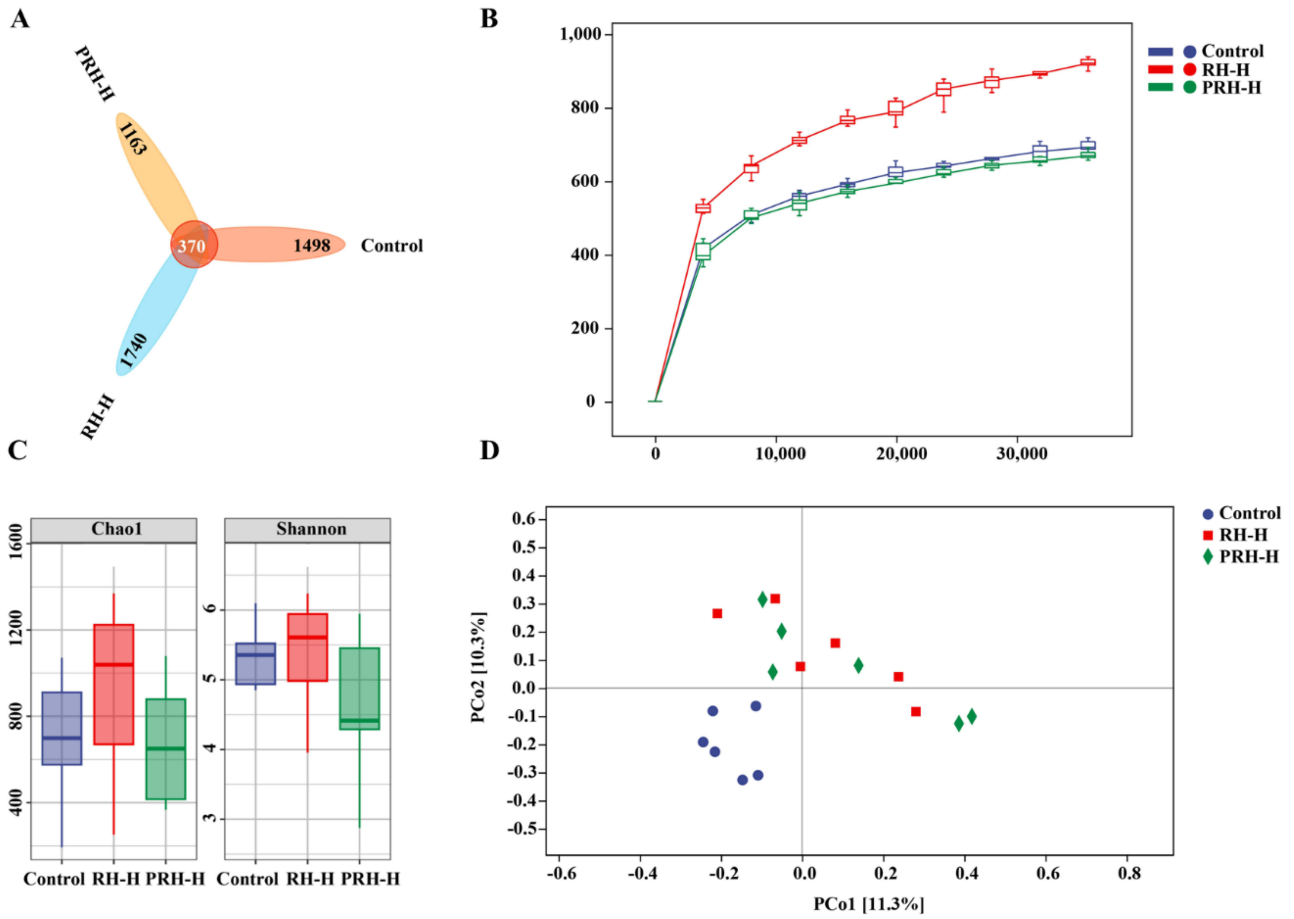

Figure 5 ASV/OTU diagram (**A**) rarefaction curve of samples (**B**) alpha diversity estimators (**C**) beta diversity estimators (**D**).

Metabolomics Analysis

Serum samples were separated using UPLC-MS (positive and negative modes; Figures S4 and S5), and the data from serum samples were analyzed using principal component analysis (PCA) and partial least squares discriminant analysis (PLS-DA). A distinct separation between the control and administration groups was evident in the PCA and PLS-DA score plots (Figure 7), indicating a clear distinction between these groups.

Potential metabolites were screened and identified using the Human Metabolome Database (http://www.hmdb.ca/) and the Kyoto Encyclopedia of Genes and Genomes (http://www.genome.jp/kegg/) (Table 1), and the volcano plot of the differential metabolites between the control and RH-H groups is shown in Figure 7. The screening criteria were as follows: $p<0.05$, VIP≥1, fold change (FC)≤0.833 or ≥1.2 (control vs RH-H).[22,28] Compared to the control group, among the 35 potential metabolites (1–21, positive ion mode; 22–35, negative ion mode), the levels of (R)-lipoic acid, cephalosporin C, and phosphatidylglycerol (PG) (13:0/18:0) were significantly upregulated in the RH-H group, while other metabolites were significantly downregulated.

Additionally, as shown in Table S1, the levels of upregulated metabolites in the PRH-H group were lower than those in the RH-H group, and the levels of downregulated metabolites in the PRH-H group were higher than those in the RH-H group, indicating that the effect of PRH on potential metabolites was less than that of RH.

The related metabolic pathways were analyzed using Metabolomics Pathway Analysis (http://www.metaboanalyst.ca/). The results of detailed metabolic pathway analysis are presented in Figure 7 and Table S2, showing notable perturbations in glycerophospholipid metabolism.

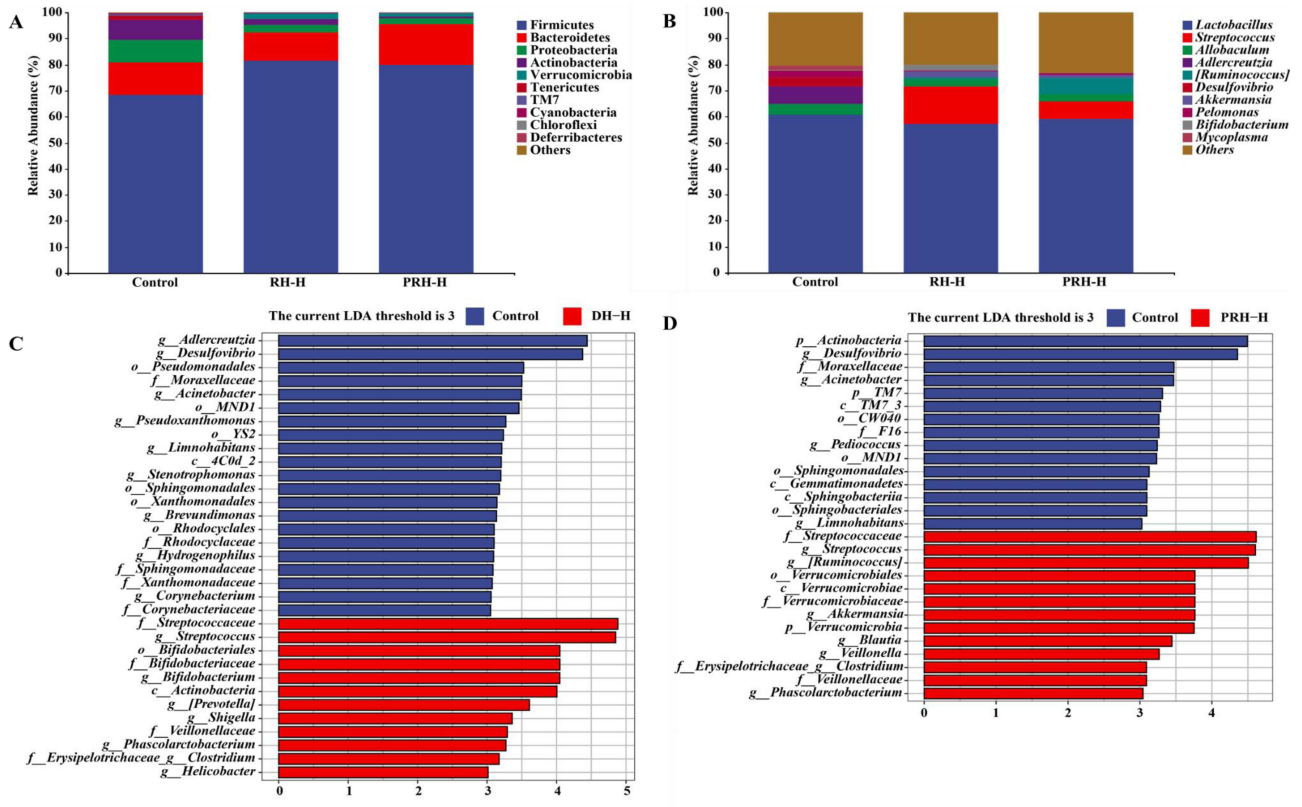

Figure 6 Relative abundance of microbial community in each group at the phylum level (**A**) and genus level (**B**) the difference of RH and PRH on GM in mice by LEfSe analysis (**C** and **D**).

Anthraquinone/Anthrone Content

The UPLC-MS chromatograms of standard solutions, RH, and PRH are shown in Figures S6–S8. The mass parameters and ion transitions of anthraquinones/anthrones were presented in Table S3. The linear relationships are listed in Table S4. The precision, stability, and repeatability were lower than 3%, and the recoveries ranged from 98.32% to 102.67% with average RSD values lower than 3% (Table S5), indicating that the method was accurate and successful. Compared with RH, the contents of anthraquinones and anthrones were clearly decreased in PRH (Table 2), and the decreased ratio from 11.34 to 71.28.

Correlation Analysis

Correlation analysis of GM, inflammatory factors, occludin, and ZO-1 suggested a significant positive correlation between *Streptococcus* and inflammatory factors (TNF-α, IL-6, and IFN-γ) at the genus level, and there was a significant negative correlation between *Streptococcus* and occludin and ZO-1. In addition, a negative correlation between *Lactobacillus* and IL-6 levels was observed, although it was not statistically significant (Figure 8A).

Correlation analysis between GM and potential metabolites showed a negative correlation between *Streptococcus* and the upregulated metabolites (1, 5, and 9) without significant differences at the genus level, while a significant positive correlation was found between *Streptococcus* and the downregulated metabolites (except for 7, 14, 18, 22, 23, 25, 26, 27, 30, and 31) (Figure 8B).

Discussion

Existing studies have confirmed that GM plays a role in the occurrence and development of diarrhea.[29,30] Therefore, research on GM is conducive to elucidating the mechanism of diarrhea. Previous studies have shown that probiotics, such as *Lactobacillus*, help metabolize undigested carbohydrates to produce short-chain fatty acids, thereby reducing the

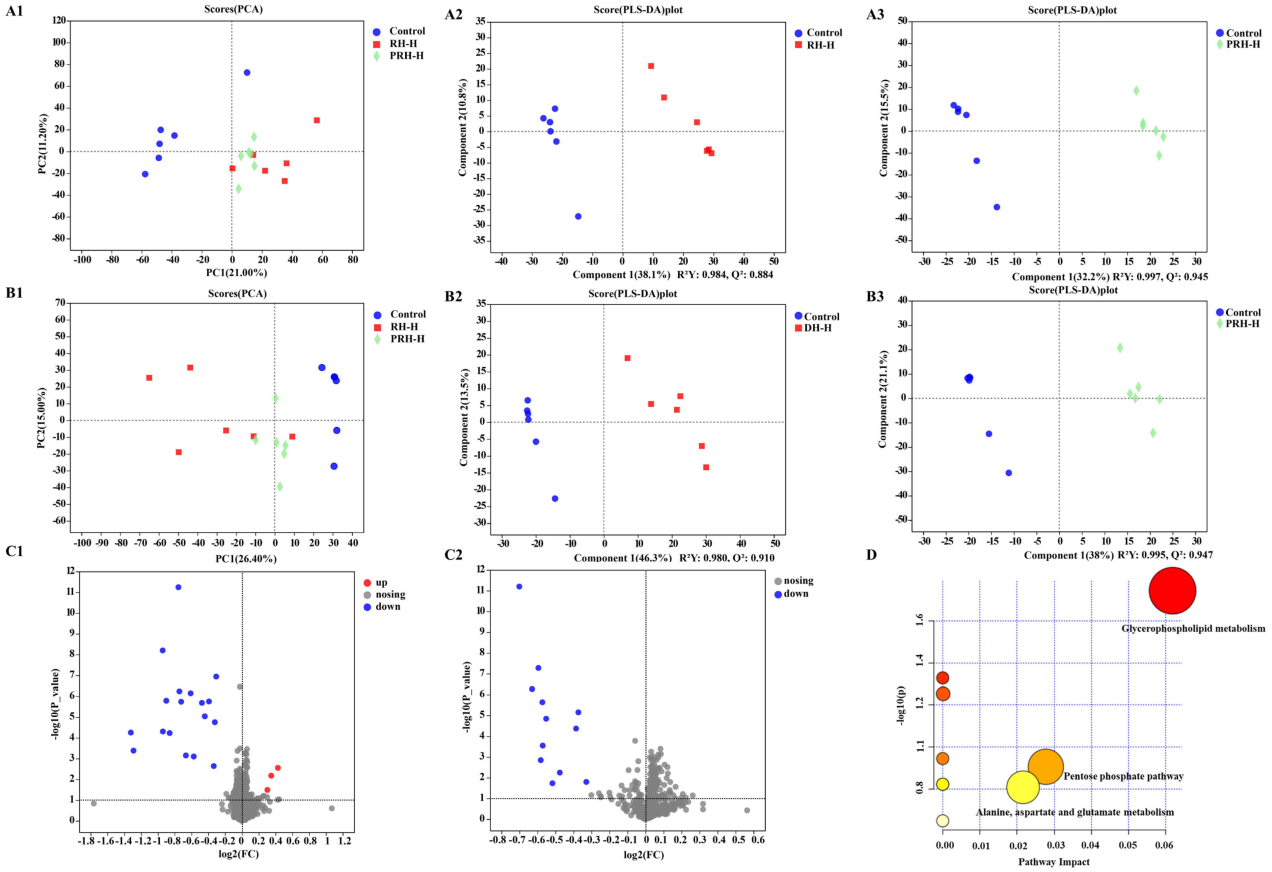

Figure 7 PCA scores plots (**A1** and **B1**) and PLS-DA scores plots (**A2-A3**, **B2-B3**) of serum samples from control, RH-H and PRH-H groups (**A**) positive, (**B**) negative. The volcano plot between control group and RH-H (**C1**) positive, (**C2**) negative, the result of detailed metabolic pathways analysis (**D**).

incidence of diarrhea.[31] In addition, the abundance of pathogenic bacteria, such as *Streptococcus* and *Shigella*, increases with diarrhea.[32] In the present study, the abundance of *Lactobacillus* decreased, while the abundance of *Streptococcus* and *Shigella* increased in the RH-H administration group, which was accompanied by evident diarrhea. In contrast, GM remained at normal levels in the PRH-H administration group. These results indicate that RH can cause diarrhea and GM dysbiosis, while PRH has a less severe impact than RH.

The intestinal barrier plays a crucial role in the interaction between the host and the external environment and prevents the transfer of bacteria and endotoxins to extraintestinal sites, thereby preventing the occurrence of diarrhea.[33] The intestinal barrier is established by tight junctions of intestinal epithelial cells, composed of several membrane-

Table 1 Identification Results of Potential Serum Metabolites (n=6, Control Vs RH-H)

No	Metabolite	FC	VIP	Up/Down	KEGG	KEGG Map
1	(R)-Lipoic acid	1.234	1.555	Up	C16241	map01100; map00785
2	Salicylaldehyde	0.655	2.864	Down	C06202	map01100
3	Aflatoxin G1	0.672	2.437	Down	C16755	map01100
4	4-coumaroylshikimate	0.736	2.678	Down	C02947	map01100
5	Cephalosporin C	1.345	2.122	UP	C00916	map01100
6	Luteolin	0.536	3.367	Down	C01514	map01100
7	Coniferaldehyde	0.762	2.229	Down	C02666	map01100
8	Sn-glycero-3-Phosphoethanolamine	0.606	2.929	Down	C01233	map00565; map00564
9	PG(13:0/18:0)	1.274	1.916	Up	C00344	map01100; map00564

(*Continued*)

Table 1 (Continued).

No	Metabolite	FC	VIP	Up/Down	KEGG	KEGG Map
10	Gentisic acid	0.520	3.639	Down	C00628	map01100; map00350
11	Pretyrosine	0.400	3.585	Down	C00826	map01100; map00400; map01230
12	Isopropylmaleic acid	0.719	2.563	Down	C02631	map01210; map00290
13	Hydroxyphenylacetylglycine	0.800	2.126	Down	C05596	map00350
14	7-Methylxanthosine	0.592	3.525	Down	C16352	map01100; map00232
15	Apigenin	0.793	2.087	Down	C01477	map01100
16	Salidroside	0.521	3.905	Down	C06046	map01100; map00350
17	Ascorbic Acid	0.551	2.771	Down	C01041	map01100; map00053
18	Genistein	0.409	3.268	Down	C06563	map01100

Table 2 Determination of the Eleven Components in Samples of RH and PRH (n = 6)

Compounds	RH	PRH	Changes (%)
	Average contents (ug/g)	Average contents (ug/g)	
1	2188.64±240.55	628.38±179.93	−71.28
2	5148.78±287.96	4212.38±317.47	−18.18
3	737.19±53.34	436.09±46.29	−40.84
4	339.21±11.21	300.74±10.05	−11.34
5	3030.14±84.82	2046.95±109.92	−32.44
6	594.92±20.48	429.85±10.69	−27.74
7	1188.11±21.24	878.71±15.06	−26.04
8	872.53±32.97	673.1±32.73	−22.85
9	223.99±7.27	124.14±15.4	−44.57
10	373.55±16.45	182.73±6.67	−51.08

associated proteins, including ZO-1 and occludin.[34] Recent research has indicated that dysregulated GM, such as increased *Escherichia coli* and decreased *Lactobacillus*, can cause abnormal expression of ZO-1 and occludin, promoting intestinal permeability and damaging the intestinal barrier.[13,35] For example, Zhou et al found that the GM metabolite butyrate promoted the recovery of the intestinal barrier by upregulating ZO-1 levels in a steatohepatitis model.[36] Furthermore, Gan et al found that the downregulation of ZO-1 and occludin increased intestinal barrier permeability and induced the infiltration of inflammatory factors, showing a significant positive correlation between the disruption of intestinal barrier function and inflammatory factors (TNF-α and IFN-γ).[37] In the present study, RH and PRH reduced the expression of occludin and ZO-1. Combined with the results of correlation analysis (Figure 8A), these findings indicate that RH and PRH may alter GM composition, leading to the disruption of intestinal barrier function.

GM is not only necessary for immune homeostasis but also affects the host's regulation of immune diseases.[38] Research indicates that *E. coli* and *Streptococcus* can induce T regulatory cells (Treg) in the lamina propria of the small intestine. The activation and overexpression of Treg can further lead to the release of inflammatory cytokines, such as IFN-γ and IL-17.[39] Additionally, studies have found that GM activates immune cells and induces the production of inflammatory factors through short-chain fatty acids (SCFAs), including acetic acid, propionic acid, and butyric acid. SCFAs help regulate intestinal homeostasis, activate T cells, and induce TNF-α production. They can also affect IL-6 and TNF-α production in monocytes, myeloid dendritic cells, and plasmacytoid dendritic cells. Propionate and butyrate could inhibit the production of IFN-γ.[40] The reduction of *Lactobacillus* can lead to increased production of TNF-α and IFN-γ, inducing IL-6 and IL-23 to immerse in T helper cells 17, thereby inducing inflammatory responses.[41] The increase in the abundance of *Shigella* aligns with elevated IL-6 levels.[42] The current study showed that TNF-α, IL-6, and IFN-γ levels increased in both the RH and PRH groups (Figure 8A). Combined with the IHC and correlation analyses, these results indicate that RH and PRH may increase intestinal permeability, leading to the release of TNF-α, IL-6, and IFN-γ.

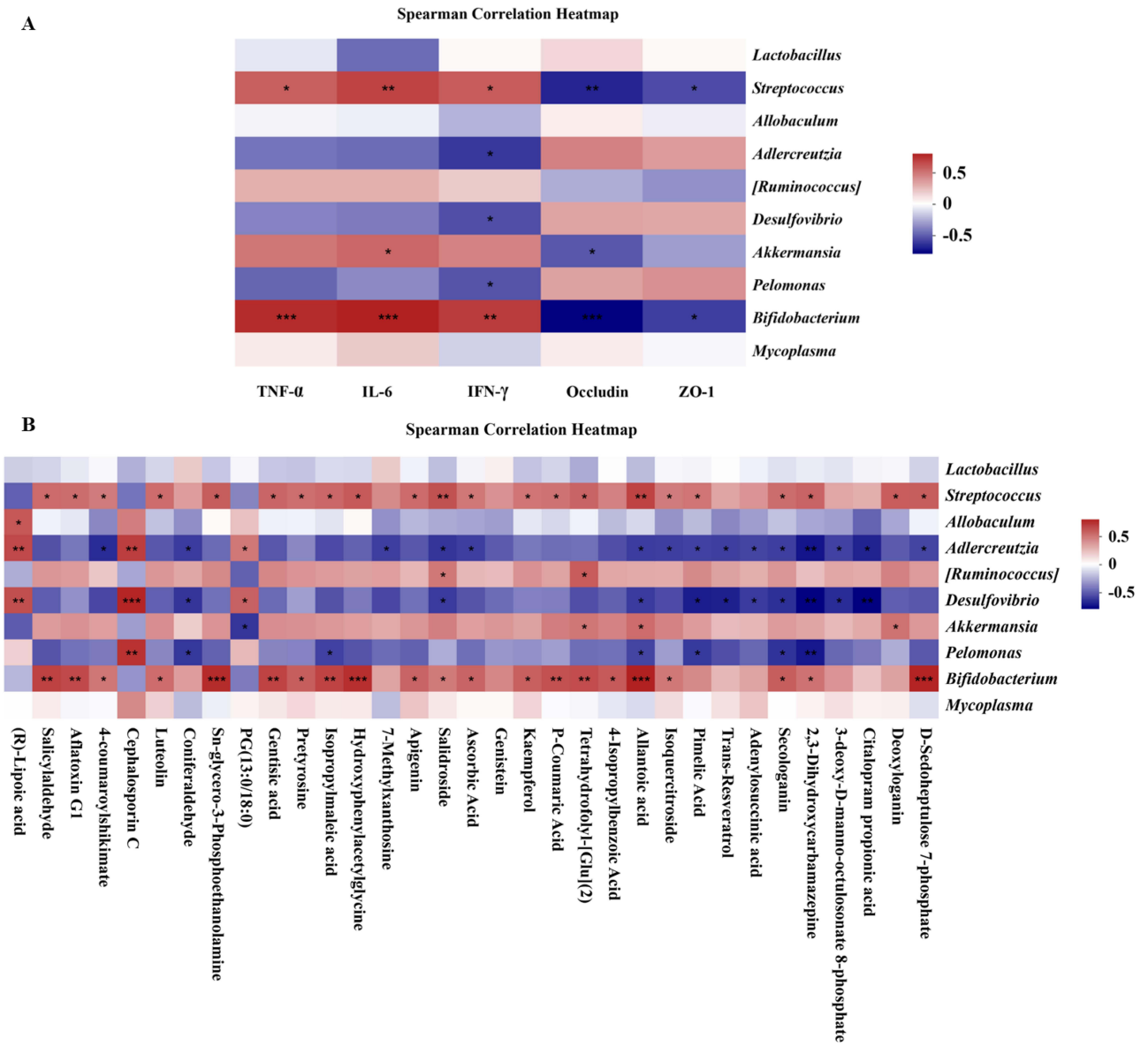

Figure 8 Correlation analysis of GM with inflammatory factors, occludin and ZO-1 (**A**) correlation analysis of GM with potential metabolites (**B**) *$p < 0.05$, **$p < 0.01$, ***$p < 0.001$.

Notable perturbations in amino acid and glycerophospholipid metabolism have been observed in previous studies on inflammatory bowel disease, and these alterations may exacerbate disease progression.[43,44] Interestingly, our study found significant perturbations in glycerophospholipid metabolism after RH administration, with two metabolites, sn-glycero-3-phosphoethanolamine and PG (13:0/18:0), being related to glycerophospholipid metabolism. Several studies have demonstrated that 1-acyl-sn-glycero-3-phosphoethanolamine and 1-octadecanoyl-2-(4z,7z,10z,13z,16z,19z-docosahexaenoyl)-sn-glycero-3-phosphoethanolamine, which have a nuclear structure similar to sn-glycero-3-phosphoethanolamine, are markedly downregulated in inflammatory diseases.[45] The glycerophospholipid molecules are mainly phosphatidylethanolamine (PE), PG, and phosphatidylcholine (PC). The increased levels of PEs, PGs, and PCs can be used as potential biomarkers for intestinal injury and proinflammatory activity.[24,46] The current study demonstrated that sn-glycero-3-phosphoethanolamine levels decreased, while PG (13:0/18:0) levels increased in the RH-H group; however, these changes were alleviated after PRH treatment. These results indicate that changes in sn-glycero-3-phosphoethanolamine and PG (13:0/18:0) levels may be associated with RH-induced diarrhea.

The main chemical components of RH include anthraquinones, anthrones, stilbenes, phenylbutanones, chromogens, flavonoids, flavanols, and tannins. Studies have shown that anthraquinones and anthrones in RH possess purgative effects.[15,47] In the determination of the chemical constituents of RH and PRH, the anthraquinone and anthrone contents in PRH showed different decreasing trends, which may be the key substances that alleviate diarrhea. In summary, the long-term use of RH can cause diarrhea, accompanied by GM imbalances, the release of inflammatory factors, and the downregulation of ZO-1 and occludin expression, which, in turn, leads to increased intestinal barrier permeability. Correlation analysis between GM and its metabolites showed that *Streptococcus* was significantly positively correlated with sn-glycero-3-phosphoethanolamine (Figure 8B). The anthraquinone and anthrone content in RH decreased after wine steaming. PRH mitigated this effect by balancing GM dysbiosis, restoring ZO-1 and occludin levels, reducing the release of inflammatory factors, and inhibiting the increase in intestinal barrier permeability. Simultaneously, the decrease in anthraquinone content may underlie the mechanism and material basis by which diarrhea is relieved after RH steaming.

The results of the current study showed that RH can cause diarrhea by affecting the abundance of *Lactobacillus, Shigella*, and *Streptococcus*, leading to impaired intestinal barrier function and the release of inflammatory factors. However, this study only evaluated intestinal barrier function, inflammatory factor levels, GM composition, and correlation analyses. Although the mechanism by which wine steaming alleviates RH-induced diarrhea is hypothesized, causal relationships have not been established. Therefore, subsequent research must be conducted using metagenomic sequencing technology to analyze the changes in GM after RH and PRH administration, and differential strains must be screened. The effects of different bacterial genera on immune and intestinal barrier functions can be verified. This would

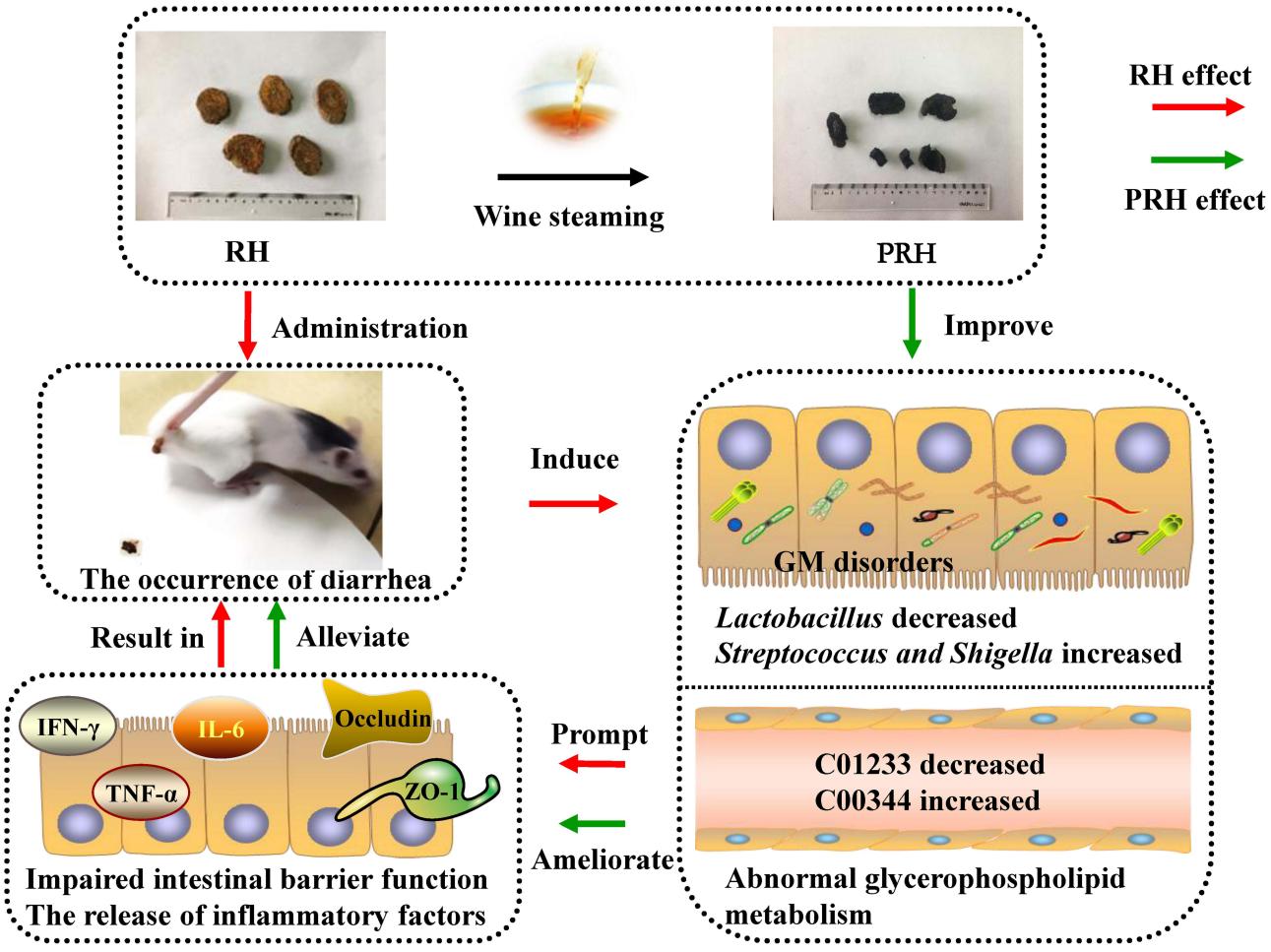

Figure 9 The potential mechanism of wine steaming in alleviating the diarrhea of RH.

confirm the relationship between RH-induced diarrhea and changes in GM and immune function. Additionally, blood component analysis can also be carried out to explore whether they are related to a decrease in anthraquinone content.

Conclusion

In this study, 33 potential marker metabolites of diarrhea caused by RH were identified, including sn-glycero-3-phosphoethanolamine and PG (13:0/18:0), as well as significant perturbations in glycerophospholipid metabolism. Collectively, these results indicate that RH can cause GM disorders and abnormal glycerophospholipid metabolism, promote impaired intestinal barrier function, and lead to the release of inflammatory factors, ultimately resulting in diarrhea. PRH can partly restore disorders in the GM, improve abnormal glycerophospholipid metabolism, repair the gut barrier, and alleviate inflammation, thereby relieving diarrhea (Figure 9). This study contributes to our understanding of the mechanisms by which wine steaming alleviates RH-induced diarrhea and provides a reference for the safe and rational use of RH in clinical practice.

Author Contributions

All authors made a significant contribution to the work reported, whether that is in the conception, study design, execution, acquisition of data, analysis and interpretation, or in all these areas; took part in drafting, revising or critically reviewing the article; gave final approval of the version to be published; have agreed on the journal to which the article has been submitted; and agree to be accountable for all aspects of the work.

Funding

The authors gratefully acknowledged the National Natural Science Foundation of China (82104396, 81973592, 81903786), Subject Innovation Team of Shaanxi University of Chinese Medicine (2019-YL10), Scientific Research Project of Shaanxi Administration of traditional Chinese Medicine (2021-ZZ-JC012), and Scientific Research Project of Education Department of Shaanxi Provincial Government (21JK0592), Key Disciplines of High-level Traditional Chinese Medicine in Shaanxi Province for Science of Chinese Medicinal Preparation.

Disclosure

The authors have no conflicts of interest in this work.

References

1. Zhang L, Yan J, Liu X, et al. Pharmacovigilance practice and risk control of traditional Chinese medicine drugs in China: current status and future perspective. *J Ethnopharmacol*. 2012;140(3):519–525. doi:10.1016/j.jep.2012.01.058
2. Chen JQ, Li DW, Chen YY, et al. Elucidating dosage-effect relationship of different efficacy of rhubarb in constipation model rats by factor analysis. *J Ethnopharmacol*. 2019;238:111868. doi:10.1016/j.jep.2019.111868
3. Liu J, Wang WF, Cheng P. A song of ice and fire: cold and hot properties of traditional Chinese medicines. *Front Pharmacol*. 2021;11:598744. doi:10.3389/fphar.2020.598744
4. Lin XY, Tian XH, Huang XM, et al. Material basis of Rhei Radix et Rhizoma-Coptidis Rhizoma combination in alleviating "bitter-cold" properties based on supramolecular chemistry of Chinese medicine. *China J Chin Mater Med*. 2022;47(22):6066–6075. doi:10.19540/j.cnki.cjcmm.20210401.303
5. Zhang Q, Zhao CB, Song YJ, et al. Effect of *Rhei Radix et Rhizoma* before and after steaming with wine on serum inflammatory factors and gut microbiota in normal mice. *J Shaanxi Univ Chin Med*. 2023;46(2):43–52. doi:10.13424/j.cnki.jsctcm.2023.02.007
6. Commission CP. *Pharmacopoeia of the People's Republic of China*. Vol. 1. Beijing: China Medical Science Press; 2020:24–25.
7. He G, Wang X, Liu W, et al. Chemical constituents, pharmacological effects, toxicology, processing and compatibility of Fuzi (lateral root of Aconitum carmichaelii Debx): a review. *J Ethnopharmacol*. 2023;307:116160. doi:10.1016/j.jep.2023.116160
8. Zhang Q, Li ZL, Zhang Y, et al. Effect of the vinegar-process on chemical compositions and biological activities of Euphorbia kansui: a review. *J Ethnopharmacol*. 2020;252:112557. doi:10.1016/j.jep.2020.112557
9. Hou A, Lv J, Zhang S, et al. Salt processing: a unique and classic technology for Chinese medicine processing. *Front Pharmacol*. 2023;14:1116047. doi:10.3389/fphar.2023.1116047
10. Zhu T, Liu X, Wang X, et al. Profiling and analysis of multiple compounds in rhubarb decoction after processing by wine steaming using UHPLC-Q-TOF-MS coupled with multiple statistical strategies. *J Sep Sci*. 2016;39(15):3081–3090. doi:10.1002/jssc.201600256
11. Hu LQ, Wang YQ, Sun HJ, et al. An untargeted metabolomics approach to investigate the wine-processed mechanism of Scutellariae radix in acute lung injury. *J Ethnopharmacol*. 2020;253:112665. doi:10.1016/j.jep.2020.112665

12. Zhang ZK, Zheng YJ, Zhang BX, et al. Untargeted serum and gastric metabolomics and network pharmacology analysis reveal the superior efficacy of zingiberis rhizoma recens-/euodiae fructus-processed Coptidis Rhizoma on gastric ulcer rats. *J Ethnopharmacol*. 2024;332:118376. doi:10.1016/j.jep.2024.11837
13. Zhang Q, Chen YY, Yue SJ, et al. Research progress on processing history evolution as well as effect on chemical compositions and traditional pharmacological effects of Rhei Radix et Rhizoma. *China J Chin Mater Med*. 2021;46(3):539–551. doi:10.19540/j.cnki.cjcmm.20201105.601
14. Wang Y, Zhang X, Ma YL, et al. Advances in processing, pharmacodynamics and clinical application of prepared Rhei Radix et Rhizoma. *Chin J Exp Tradit Med*. 2018;24(24):219–226. doi:10.13422/j.cnki.syfjx.20182408
15. Yang XR, Dai LX, Yan FY, et al. The phytochemistry and pharmacology of three Rheum species: a comprehensive review with future perspectives. *Phytomedicine*. 2024;131:155772. doi:10.1016/j.phymed.2024.15577
16. Fan L, Qi Y, Qu S, et al. *B. adolescentis* ameliorates chronic colitis by regulating Treg/Th2 response and gut microbiota remodeling. *Gut Microbes*. 2021;13(1):1–17. doi:10.1080/19490976.2020.1826746
17. Li Y, Xia S, Jiang X, et al. Gut microbiota and diarrhea: an updated review. *Front Cell Infect Microbiol*. 2021;11:625210. doi:10.3389/fcimb.2021.625210
18. Zhong T, Wang Y, Wang XA, et al. Diarrhea in suckling lambs is associated with changes in gut microbiota, serum immunological and biochemical parameters in an intensive production system. *Front Microbiol*. 2022;13:1020657. doi:10.3389/fmicb.2022.1020657
19. Zhang Q, Bai Y, Wang W, et al. Role of herbal medicine and gut microbiota in the prevention and treatment of obesity. *J Ethnopharmacol*. 2023;305:116127. doi:10.1016/j.jep.2022.116127
20. Yue SJ, Wang WX, Yu JG, et al. Gut microbiota modulation with traditional Chinese medicine: a system biology-driven approach. *Pharmacol Res*. 2019;148:104453. doi:10.1016/j.phrs.2019.104453
21. Zhang Q, Yue SJ, Chen YY, et al. Research progress on traditional Chinese medicine regulating gut microbiota in treatment of chronic diarrhea. *Chin Tradit Herb Drugs*. 2022;53(8):2539–2549. doi:10.7501/j.issn.0253-2670.2023.17
22. Zheng Y, Wang J, Wang J, et al. Gut microbiota combined with metabolomics reveal the mechanism of curcumol on liver fibrosis in mice. *Biomed Pharmacother*. 2022;152:113204. doi:10.1016/j.biopha.2022.113204
23. Zhang CE, Yu XH, Cui YT, et al. Shengjiang Xiexin Decoction ameliorates antibiotic-associated diarrhea by altering the gut microbiota and intestinal metabolic homeostasis. *Phytomedicine*. 2023;113:154737. doi:10.1016/j.phymed.2023.154737
24. Zhang Q, Ju YH, Zhang Y, et al. The water expelling effect evaluation of 3-*O*-(2'*E*,4'*Z*-Decadi-enoyl)-20-*O*-acetylingenol and ingenol on H22 mouse hepatoma ascites model and their content differences analysis in Euphorbia kansui before and after stir-fried with vinegar by UPLC. *J Ethnopharmacol*. 2021;267:113507. doi:10.1016/j.jep.2020.113507
25. de Vos WM, Tilg H, Van hul M, et al. Gut microbiome and health: mechanistic insights. *Gut*. 2022;71(5):1020–1032. doi:10.1136/gutjnl-2021-326789
26. Li YQ, Sun XQ, Liu XN, et al. P2X7R-NEK7-NLRP3 inflammasome activation: a novel therapeutic pathway of Qishen Granule in the treatment of acute myocardial ischemia. *J Inflamm Res*. 2022;15:5309–5326. doi:10.2147/JIR.S37396
27. Zhang Q, Zhang Y, Zhou SK, et al. Toxicity reduction of *Euphorbia kansui* stir-fried with vinegar based on conversion of 3-*O*-(2'*E*,4'*Z*-Decadi-enoyl)-20-*O*-acetylingenol. *Molecules*. 2019;24(20):3806. doi:10.3390/molecules24203806
28. Sreekumar A, Poisson LM, Rajendiran TM, et al. Metabolomic profiles delineate potential role for sarcosine in prostate cancer progression. *Nature*. 2009;457(7231):910–914. doi:10.1038/nature07762
29. Qu Q, Yang F, Zhao C, et al. Effects of fermented ginseng on the gut microbiota and immunity of rats with antibiotic-associated diarrhea. *J Ethnopharmacol*. 2021;267:113594. doi:10.1016/j.jep.2020.113594
30. Yang B, Yue Y, Chen Y, et al. *Lactobacillus plantarum* CCFM1143 alleviates chronic diarrhea *via* inflammation regulation and gut microbiota modulation: a double-blind, randomized, placebo-controlled study. *Front Immunol*. 2021;12:746585. doi:10.3389/fimmu.2021.746585
31. Markowiak-Kopeć P, Śliżewska K. The effect of probiotics on the production of short-chain fatty acids by human intestinal microbiome. *Nutrients*. 2020;12(4):1107. doi:10.3390/nu12041107
32. Gomez DE, Li L, Goetz H, et al. Calf diarrhea is associated with a shift from obligated to facultative anaerobes and expansion of lactate-producing bacteria. *Front Vet Sci*. 2022;9:846383. doi:10.3389/fvets.2022.846383
33. Wang T, Yao W, Li J, et al. Dietary garcinol supplementation improves diarrhea and intestinal barrier function associated with its modulation of gut microbiota in weaned piglets. *J Anim Sci Biotechnol*. 2020;11:12. doi:10.1186/s40104-020-0426-6
34. Costantini TW, Deree J, Loomis W, et al. Phosphodiesterase inhibition attenuates alterations to the tight junction proteins occludin and ZO-1 in immunostimulated Caco-2 intestinal monolayers. *Life Sci*. 2009;84(1–2):18–22. doi:10.1016/j.lfs.2008.10.00
35. Larabi A, Barnich N, Nguyen HTT. New insights into the interplay between autophagy, gut microbiota and inflammatory responses in IBD. *Autophagy*. 2020;16(1):38–51. doi:10.1080/15548627.2019.1635384
36. Zhou D, Pan Q, Xin FZ, et al. Sodium butyrate attenuates high-fat diet-induced steatohepatitis in mice by improving gut microbiota and gastrointestinal barrier. *World J Gastroenterol*. 2017;23(1):60–75. doi:10.3748/wjg.v23.i1.60
37. Gan Y, Ai G, Wu J, et al. Patchouli oil ameliorates 5-fluorouracil-induced intestinal mucositis in rats via protecting intestinal barrier and regulating water transport. *J Ethnopharmacol*. 2020;250:112519. doi:10.1016/j.jep.2019.112519
38. Brown EM, Kenny DJ, Xavier RJ. Gut microbiota regulation of T cells during inflammation and autoimmunity. *Annu Rev Immunol*. 2019;37:599–624. doi:10.1146/annurev-immunol-042718-041841
39. Geva-Zatorsky N, Sefik E, Kua L, et al. Mining the human gut microbiota for immunomodulatory organisms. *Cell*. 2017;168(5):928–943.e11. doi:10.1016/j.cell.2017.01.022
40. Porbahaie M, Hummel A, Saouadogo H, et al. Short-chain fatty acids inhibit the activation of T lymphocytes and myeloid cells and induce innate immune tolerance. *Benef Microbes*. 2023;14(4):401–419. doi:10.1163/18762891-20220113
41. Gerassy-Vainberg S, Blatt A, Danin-Poleg Y, et al. Radiation induces proinflammatory dysbiosis: transmission of inflammatory susceptibility by host cytokine induction. *Gut*. 2018;67(1):97–107. doi:10.1136/gutjnl-2017-313789
42. Li S, Zhuge A, Wang K, et al. Ketogenic diet aggravates colitis, impairs intestinal barrier and alters gut microbiota and metabolism in DSS-induced mice. *Food Funct*. 2021;12(20):10210–10225. doi:10.1039/d1fo02288a
43. Hua YL, Ma Q, Zhang XS, et al. Pulsatilla decoction can treat the dampness-heat diarrhea rat model by regulating glycerinphospholipid metabolism based lipidomics approach. *Front Pharmacol*. 2020;11:197. doi:10.3389/fphar.2020.00197

44. Lee JS, Kim SY, Chun YS, et al. Characteristics of fecal metabolic profiles in patients with irritable bowel syndrome with predominant diarrhea investigated using ^{1}H-NMR coupled with multivariate statistical analysis. *Neurogastroenterol Motil*. 2020;32(6):e13830. doi:10.1111/nmo.13830
45. Jeyaraj EJ, Han ML, Li J, et al. Metabolic perturbations and key pathways associated with the bacteriostatic activity of *Clitoria ternatea* flower anthocyanin fraction against *Escherichia coli*. *Access Microbiol*. 2023;5(6):000535.v5. doi:10.1099/acmi.0.000535.v5
46. Xia F, Liu C, Wan JB. Characterization of the cold and hot natures of raw and processed Rehmanniae Radix by integrated metabolomics and network pharmacology. *Phytomedicine*. 2020;74:153071. doi:10.1016/j.phymed.2019.153071
47. Qin Y, Wang JB, Kong WJ, et al. The diarrhoeogenic and antidiarrhoeal bidirectional effects of rhubarb and its potential mechanism. *J Ethnopharmacol*. 2011;133(3):1096–1102. doi:10.1016/j.jep.2010.11.04